ResearchGate

See discussions, stats, and author profiles for this publication at: https://www.researchgate.net/publication/6932367

Formation of Ordered Arrays of Oriented Polyaniline Nanoparticle Nanorods

ARTICLE *in* THE JOURNAL OF PHYSICAL CHEMISTRY B · AUGUST 2005

Impact Factor: 3.3 · DOI: 10.1021/jp0503260 · Source: PubMed

CITATIONS
44

READS
26

6 AUTHORS, INCLUDING:

Haibing Xia
Shandong University
45 PUBLICATIONS **839** CITATIONS

SEE PROFILE

Available from: Haibing Xia
Retrieved on: 26 January 2016

ARTICLES

Formation of Ordered Arrays of Oriented Polyaniline Nanoparticle Nanorods

Haibing Xia,[†] Janaky Narayanan,[‡] Daming Cheng,[†] Changyong Xiao,[†] Xiangyang Liu,[‡] and Hardy Sze On Chan*[,†]

Department of Chemistry, National University of Singapore, 3 Science Drive 3, Singapore 117543, and Department of Physics, National University of Singapore, 2 Science Drive 3, Singapore 117542

Received: January 19, 2005; In Final Form: May 9, 2005

We report the preparation of ordered polyaniline (PANI) nanorod arrays in an aqueous medium. The oriented PANI nanorods (80−400 nm in diameter and 8−15 μm in length) were synthesized in the presence of hydrophilic Allura Red AC (ARAC) as the structure-directing agent and ammonium persulfate as an oxidant in HCl solution. The morphologies of the oriented PANI nanoparticle nanorods were confirmed by scanning electron microscopy (SEM) and transmission electron microscopy images, and the effect of reaction conditions on the morphology of PANI nanostructures was also studied. On the basis of the result obtained from small-angle X-ray scattering, we propose that rodlike micelle arrays of ARAC−aniline are responsible for directing the formation of oriented PANI nanoparticle nanorods. SEM images and the data analysis of static and dynamic light scattering give supportive evidence to the formation of the PANI nanoparticle nanorods by an elongation process. The chemical and electronic structures of the PANI nanorods were also studied by Fourier transform IR and UV−vis spectrometries, respectively.

Introduction

Multidimensional ordering of materials is central to synthetic materials chemistry. Direct fabrication of complex nanostructures with controlled morphology, orientation, and surface architectures remains a significant challenge.[1] Self-assembly based on selective control of noncovalent interactions (hydrogen bonding, van der Waals forces, $\pi-\pi$ stacking interaction, metal coordination, or dispersive forces) provides a powerful tool for the creation of well-defined structures at a molecular level and a means of extending such structures to macroscopic length scales.[2] The building and patterning of inorganic nanoparticles into two- and three-dimensional well-ordered structures have attracted a great deal of interest.[3−9] However, few reports have appeared describing the assembly of polymer nanoparticles into ordered nanostructures, which may be due to the difficulty in the organization of polymer nanoparticles.

Polyaniline (PANI) is a conducting polymer that has been widely studied due to its simple preparation, good thermal and environmental stability, structure versatility, and potential applications as electrical and optical materials.[10,11] Although micro- and nanostructures of PANI (tubes and particles) have been prepared by chemical and electrochemical oxidative polymerization of aniline within templates[12−14] or with structure-directing agents,[15−21] so far few publications[22] have reported on the preparation of oriented PANI nanostructures with controlled morphology.

In this article, we describe the synthesis of ordered arrays of oriented PANI nanoparticle nanorods and show the usefulness of self-assembly in generating such a novel material. The influence of the synthetic conditions on the specific morphology and size of PANI nanorods was investigated. On the basis of the results obtained from a small-angle X-ray scattering (SAXS) study, we propose that rodlike micelle arrays of Allura Red AC−aniline (ARAC−An) are responsible for directing the formation of oriented PANI nanoparticle nanorods. Scanning electron micrscopy (SEM) images and the data analysis of static light scattering (SLS) and dynamic light scattering (DLS) also support the formation of the PANI nanorods by an elongation process. The chemical and electronic structures of the PANI nanorods were also studied by Fourier transform IR (FTIR) and UV−vis spectrometries, respectively.

Experimental Section

Materials. The aniline monomer (An) was distilled under reduced pressure. Allura Red AC (ARAC) and ammonium persulfate (APS) were purchased from Sigma and used without further treatment.

Preparation of Oriented PANI Nanorod Arrays. The general polymerization process of oriented PANI nanorods is as follows: Approximately 0.25 mL (2.75 mmol) of aniline was added to 0.04 g (0.08 mmol) of ARAC in 15 mL of HCl solution (0.67 M), and the mixture was stirred for 30 min to form a solution of ARAC−An salt. When the solution was cooled to 2.5 °C, an aqueous solution of APS (0.63 g in 10 mL of distilled water) was added to the above solution. The mixture was allowed to further react for 16 h at 2.5 °C with stirring. Acetone

* Author to whom correspondence should be addressed. Phone: 65-68742833. Fax: 65-67774279. E-mail: chmcsoh@nus.edu.sg.
[†] Department of Chemistry.
[‡] Department of Physics.

10.1021/jp0503260 CCC: $30.25 © 2005 American Chemical Society
Published on Web 06/11/2005

was added to the solution to stop the reaction and to precipitate the PANI nanorods. The precipitate was filtered and thrice washed with distilled water and acetone. The powder was dried in a vacuum for 12 h at room temperature.

In an attempt to produce the best array of nanorods, a series of PANI products were prepared at different molar ratios of aniline to ARAC at fixed aniline concentrations. The effects of different aniline concentrations on the morphologies of the PANI products and the reaction temperatures on the sizes of the PANI nanorods were also investigated.

Characterization. The morphologies of the PANI nanorods were examined by field emission scanning electron microscopy (FE-SEM, JSM-6700F) and transmission electron microscopy (TEM, JSM-2010F).

The absorption spectra of the PANI products in solution were recorded with an UV−vis spectrophotometer (UV-1601PC, Shimadzu). A small amount of the product was dispersed in water by an ultrasonicator to provide a very dilute and homogeneous sample solution.

The molecular structure of the PANI−ARAC was determined by the FTIR spectrum (FTS3000, Bio-Rad Excalibur series).

SAXS measurements were carried out using a Bruker AXS NanoStar instrument employing a pinhole SAXS camera, cross-coupled Göbel mirrors, and a position-sensitive area detector. A sealed X-ray tube with a Cu anode (Kα wavelength of 1.542 Å) operating at 40 kV and 35 mA was used. The beam diameter at the sample was 200 μm, and the sample-to-detector distance was 106.5 cm. A thermostated sample holder (±0.1 °C) with a glass capillary of thickness 0.1 mm and diameter 0.78 mm was employed. The collection time was 1 h. The intensity recorded on a frame size of 1024 × 1024 pixels was integrated by the normalized bin method to obtain a plot of $I(q)$ versus q where q is the wave vector.

$$q = \frac{4\pi}{\lambda}\sin(\theta/2) \tag{1}$$

λ is the wavelength of the X-ray, and θ is the scattering angle. Due to pinhole geometry, the instrumental smearing effects are negligible. The transmission of the sample, τ, was determined using glassy carbon as the standard and the solvent as the background. The background-subtracted intensity was calculated from

$$I(q) = I_s(q) - \tau I_b(q) \tag{2}$$

where $I_s(q)$ and $I_b(q)$ are, respectively, the scattered intensities for the sample and the background. The intensity values were measured in arbitrary units and normalized to the baseline.

Static and dynamic light scattering measurements were carried out using a Brookhaven light scattering instrument with a BI9000AT correlator. A He−Ne laser (λ = 632.8 nm) from Spectra Physics (model 127, 60 mW) was used as the light source. The SLS measurements were made for scattering angles in the range from 30° to 140°, and the DLS measurement was for 90°. The sample was equilibrated at 10 ± 0.1 °C. Appropriate corrections for refraction/reflection at the cell−solution interface and volume effects were applied to SLS data using standard procedures.

Results and Discussion

Morphology. SEM pictures show that the morphologies of the PANI products change with different molar ratios of aniline to ARAC (represented by [An]/[ARAC]) at a fixed aniline concentration ([An] = 0.11 M). When [An]/[ARAC] was 75, agglomerates of particles and fibers were formed (Figure 1a). The structure and morphology of the PANI product changed significantly as the ratio was decreased. Separated PANI nanorods started to appear when [An]/ [ARAC] was 60 (Figure 1b). When [An]/[ARAC] was at a low value of 25, only nanorod clusters, which were made up of oriented single nanorods with diameters of 200−400 nm and lengths of 8−15 μm (Figure 1c), were formed in the bulk. A high-resolution TEM image further shows the presence of long nanorods, which contain disordered nanoparticle arrays. Although there are defects along the nanorods, the geometrical rod shape is preserved (Figure 2). When [An]/[ARAC] was at the lowest value of 10, nanorod clusters were still observed but with the nanorods in an aggregated and entangled form (Figure 1d).

Figure 3 shows the effects of the aniline concentration on the morphologies of the PANI products at a fixed ratio ([An]/[ARAC] = 25). When [An] was 0.05 M, a network of entangled and twisted nanofibers was formed (Figure 3a). Oriented nanorods in clusters were observed when [An] was 0.11 M (Figure 1c), which turned into entangled nanorods in clusters when [An] was increased to 0.14 M (Figure 3b). These differences can be attributed to the fact that the microenvironment for the self-assembly process is different at various concentrations of aniline and ARAC. When [An] and hence [ARAC] is very low, the resulting PANI product is similar to that obtained by normal synthesis of PANI using aniline and a strong oxidant in the presence of common mineral acids such as HCl, H_2SO_4, or H_3PO_4 as dopants.[23] When [An] is high at 0.14 M, the micelles formed by the ARAC−An are not adequately separated and oriented by stirring. Therefore, the resulting PANI nanorods are easily aggregated and entangled with each other.

Formation Mechanism of PANI Nanoparticle Nanorods. Recently, Chan et al.[22] reported that the hydrophobic moiety of the structure-directing agent was able to direct the formation of cylindrical micelles. Hassan et al.[24] reported that PANI nanoparticles were prepared in rodlike micelles by a sphere-to-rod transition in anionic sodium dodecyl sulfate (SDS) micelles with the addition of aniline hydrochloride and APS. In our system, unlike SDS, pure ARAC solution does not form micelles. However, when aniline is mixed with ARAC in the presence of HCl, ARAC−An salt is formed through an acid/base reaction. This salt can form micelles, acting as "templates" to form nanotubular/nanofibrous structures under certain conditions.[25,26] There are two hydrophilic groups (SO_3^-) lying on the two ends of the structure-directing agent, the ARAC molecule, which is different from other structure-directing agents reported earlier.[15−22] When the ratio of [An]/[ARAC] is as large as 25, aniline is in excess, and the system will consist of free aniline and ARAC−An salt micelles.[15] The protonated aniline can adsorb on the micellar surface and enhance its linear growth, and free aniline can diffuse into the center of the micelles to form the core (A, Scheme 1).[15,27] This process is aided by the thorough mixing of ARAC and aniline for 30 min before APS is added. The diffusion of aniline monomers into the hydrophilic micellar core enables the polymerization, which results in the formation of nanorods.[28] In the presence of less aniline in the core, nanotubes would be partially formed.[15,28] When APS solution is added to the ARAC−An mixture, the initial stage of polymerization can be the formation of PANI nanoparticles[29,30] due to the excess amount of protonated aniline present in the solution. The ARAC−An micelles can offer substrates for these nanoparticles to adsorb and grow. PANI nanoparticles

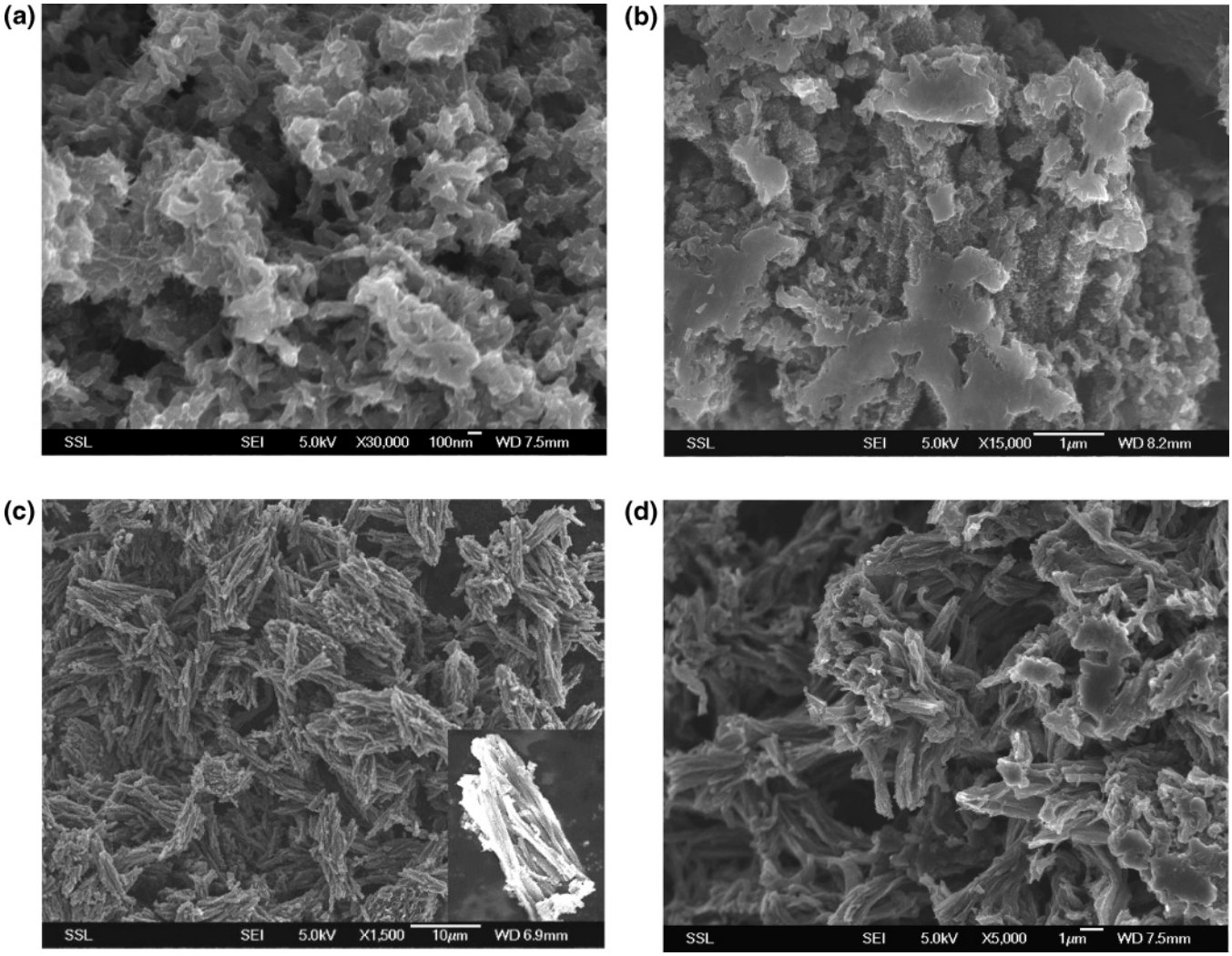

Figure 1. SEM images of PANI produced at [An]/[ARAC] values of (a) 75, (b) 60, (c) 25, and (d) 10. ([An] = 0.11 M, [An]/[APS] =1, reaction time = 16 h, temperature = 2.5 °C.)

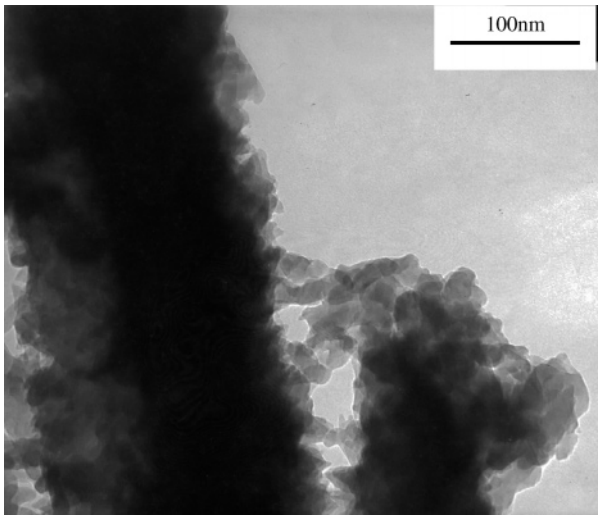

Figure 2. TEM image of PANI nanoparticle nanorods. (Sample conditions are the same as in Figure 1c.)

would aggregate on the surfaces of the rodlike micelles by interactions including hydrogen bonds and $\pi-\pi$ interactions because the surface composed of $-SO_3H$ and $-NH$ groups and phenyl rings would provide a wide variety of active sites for nucleation, organization, and the binding of nanoparticles.[29−33] The side-on attachment of the ARAC−An micelles with adsorbed nanoparticles can result in an increased diameter of the nanostructure. The end-on attachment of the micelles results in linear growth of the nanostructure. This type of reorganization is observed in organo-functionalized silica nanoparticles formed by the silica−surfactant micelles.[34] In our study, a shear flow orientation is induced by continuous stirring, which favors an end-on attachment of the micelles. Due to anisometry of the shape, the rodlike micelles tend to orient with the rod axis along the shear flow (B, Scheme 1).[35,36] Continuous stirring and polymerization result in the formation of well-oriented nanoparticle nanorods (C, Scheme 1). In one of the control experiments, when the stirring was stopped 2 min after the addition of the APS, disordered polymer rod networks were observed (Supporting Information). This confirms that extended shearing that leads to the formation of well-aligned rodlike micelle aggregates is required to obtain ordered PANI nanorod structures.

Recently, Kaner et al.[37] reported in detail the formation mechanism of PANI nanostructures. They found that if aniline monomers were polymerized by APS in acidic solution without any structure-directing agent, then PANI nanofibers or large agglomerates containing irregularly shaped particles and nanofibers would be obtained depending on the reaction conditions. In contrast to these findings, our results indicate that ARAC plays a key role in the formation of ordered nanoparticle nanorods. The reason for the formation of ordered arrays of

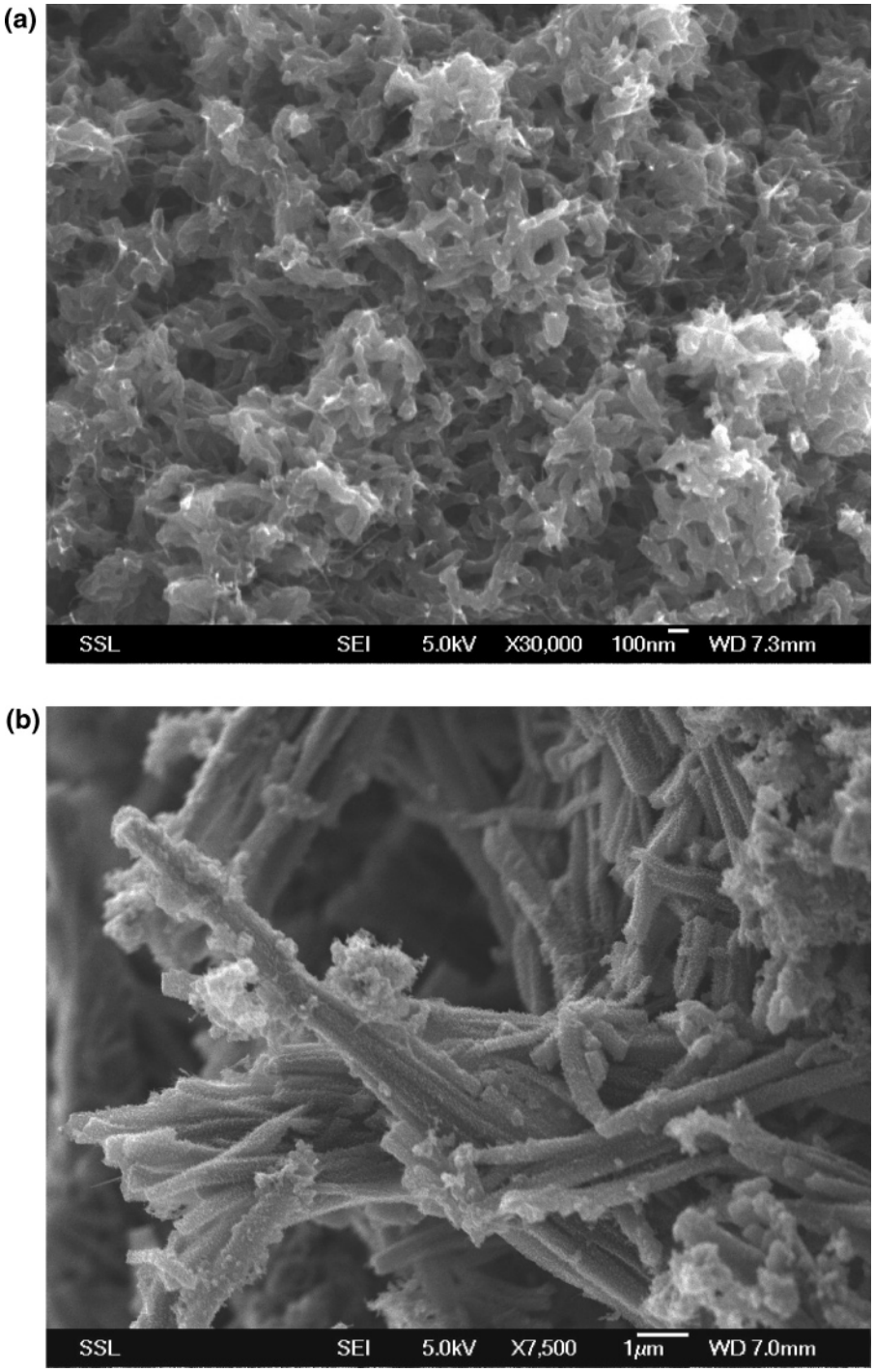

Figure 3. SEM images of PANI produced at different aniline concentrations: (a) 0.05 M; (b) 0.14 M. ([An]/[APS] = 1, [An]/[ARAC] = 25, reaction time = 16 h, temperature = 2.5 °C.)

PANI nanoparticle nanorods can be ascribed to the formation of well-aligned rodlike micelle aggregates. A great deal of PANI nanostructures without this kind of structure-directing agent have been investigated by SEM and TEM previously, but such ordered structures have never been observed.[15−21] We carried out several experiments as discussed below to confirm the proposed mechanism of formation of the nanoparticle nanorods.

To study the formation of rodlike micelles, we conducted the SAXS experiment on the aqueous (acidic) solution of ARAC−An at 2.5°C. With [An] at 0.11 M, six samples were selected with [An]/[ARAC] values of 100, 50, 33.4, 25, 20, and 16.7. The solutions were stirred thoroughly and loaded into the sample cell. During the data collection time of 1 h, the solution in the capillary remained well-dispersed. For [An]/[ARAC] = 100, the scattered intensity from the sample was very close to solvent intensity, and no meaningful data could be extracted. With progressive increases in ARAC concentration, the scattered intensity steadily increased, indicating the formation of a larger number of micelles. The SAXS intensity can be calculated as

$$I(q) = nV_p^2(\rho_p - \rho_s)^2 P(q)S(q) \qquad (3)$$

Here, n is the number of micelles per unit volume. V_p is the volume of a micelle with average scattering length density ρ_p, and ρ_s is the scattering length density of the solvent. For sufficiently dilute surfactant concentrations, the intermicellar structure factor $S(q)$ can be assumed to be unity. For rodlike micelles of length $2L$ and diameter $2R$, the form factor $P(q)$ is

SCHEME 1: Reaction Scheme for the Formation of PANI Nanoparticle Nanorods

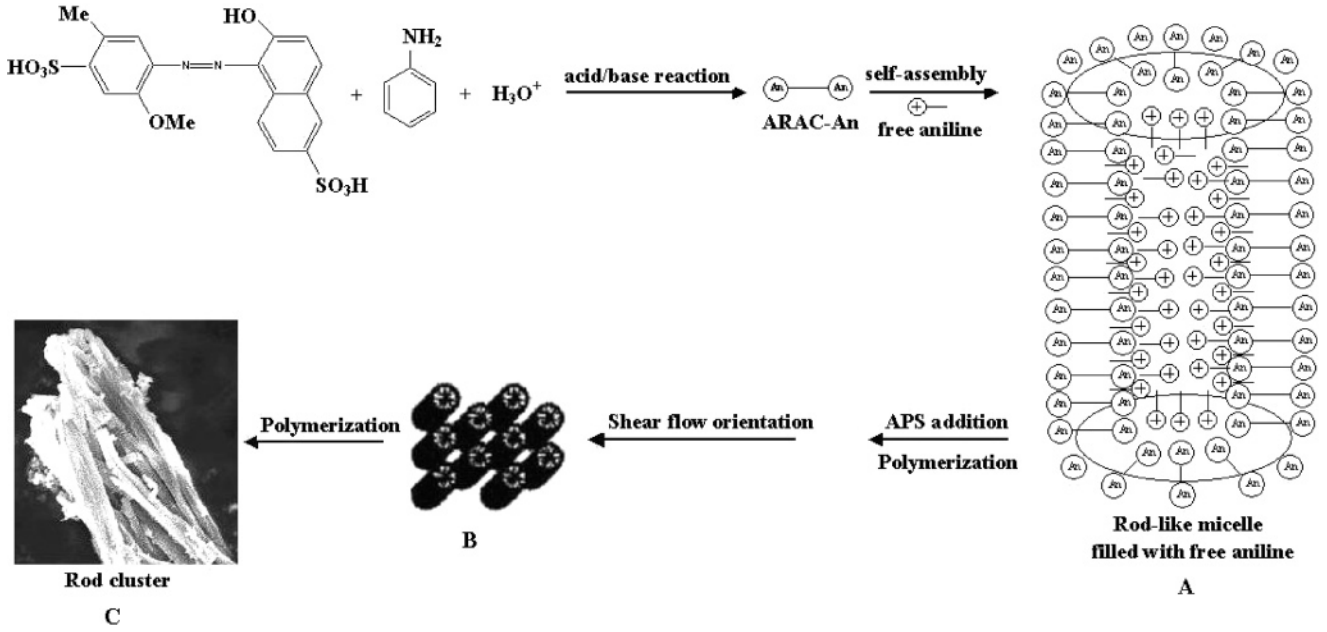

given by the following equation.[39]

$$P(q) = \int_0^{\pi/2} \left[\frac{\sin(qL\cos\beta)}{qL\cos\beta}\frac{2J_1(qR\sin\beta)}{qR\sin\beta}\right]^2 \sin\beta\, d\beta \quad (4)$$

where β defines the angular orientation between the rod axis and the wave vector. Normalizing $I(q)$ with its value at $q = 0$ gives an intensity distribution corresponding to eq 4 as $P(0) = 1$. However, as the lower limit of the wave vector, q_l, which was accessible to the experiment was not zero but finite ($q_l = 0.0092$ Å^{-1}), a scaling factor, K, was used for fitting $I(q)/I(q_l)$. Figures 4a and 4b show the SAXS intensity distribution on a log−log plot for [An]/[ARAC] values of 50 and 16.7, respectively. The theoretical curves are the form factors for rodlike micelles of diameter $2R = 260$ Å with lengths $L = 350$ and 400 Å, respectively. The scaling factor was 1.5. The data could not be fitted with a spherical shape for the micelles. Thus, in the range of [An]/[ARAC] values selected for this study, the rodlike micellar arrays of ARAC−An seem to control the formation of PANI nanoparticle nanorods.

The morphologies of the products obtained at different stages of PANI polymerization are shown in Figure 5. A small amount of the product was periodically extracted from the reaction bath for the SEM studies. The PANI extracted solution was then filtered quickly, washed by water, and dried to quench the polymerization. In the initial stage of polymerization (as soon as the solution changed from red to black), the product extracted from the solution consisted of PANI nanoparticles with an average diameter of 50 nm (Figure 5a). Figure 5b shows the PANI nanoparticle nanorods of lengths of ~1.2 μm formed after 1.5 h of reaction time. The array of oriented PANI nanoparticle nanorods formed in clusters after 4 h of reaction time is shown in Figure 5c. These SEM images taken at different reaction stages indicate that well-aligned oriented PANI nanorods are formed through the PANI nanoparticle growth by an attachment and elongation process.

To confirm the morphologies of the nanorods, we also performed the SLS and DLS measurements on PANI nanorods formed using [An]/[ARAC] = 25 with [An] = [APS] = 0.11 M after 9 h of polymerization at 2.5 °C. The solution was diluted 500 times and equilibrated at 10 °C. The intensity distribution of the SLS data for the PANI nanorods is shown in Figure 6a.

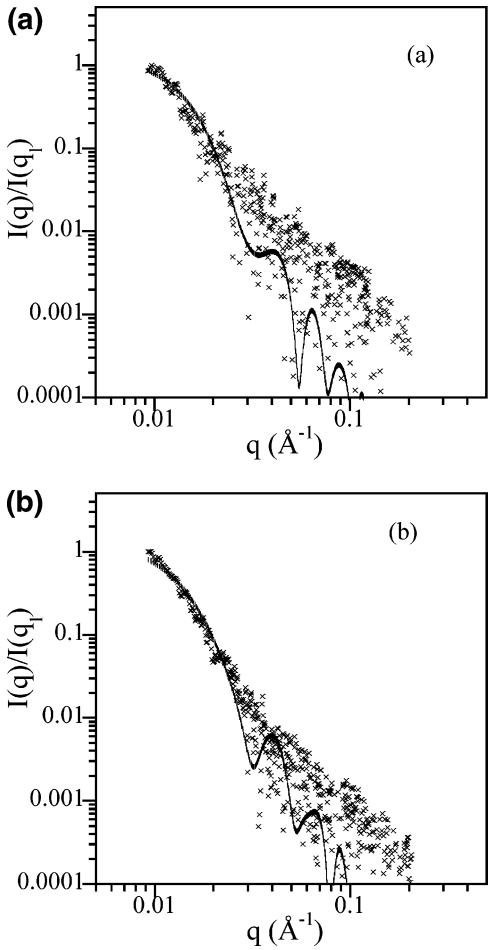

Figure 4. SAXS intensity distribution at 2.5 °C for [An]/[ARAC] values of (a) 50 and (b) 16.7. The continuous lines are the theoretical fits using eq 4 with a scaling factor of 1.5.

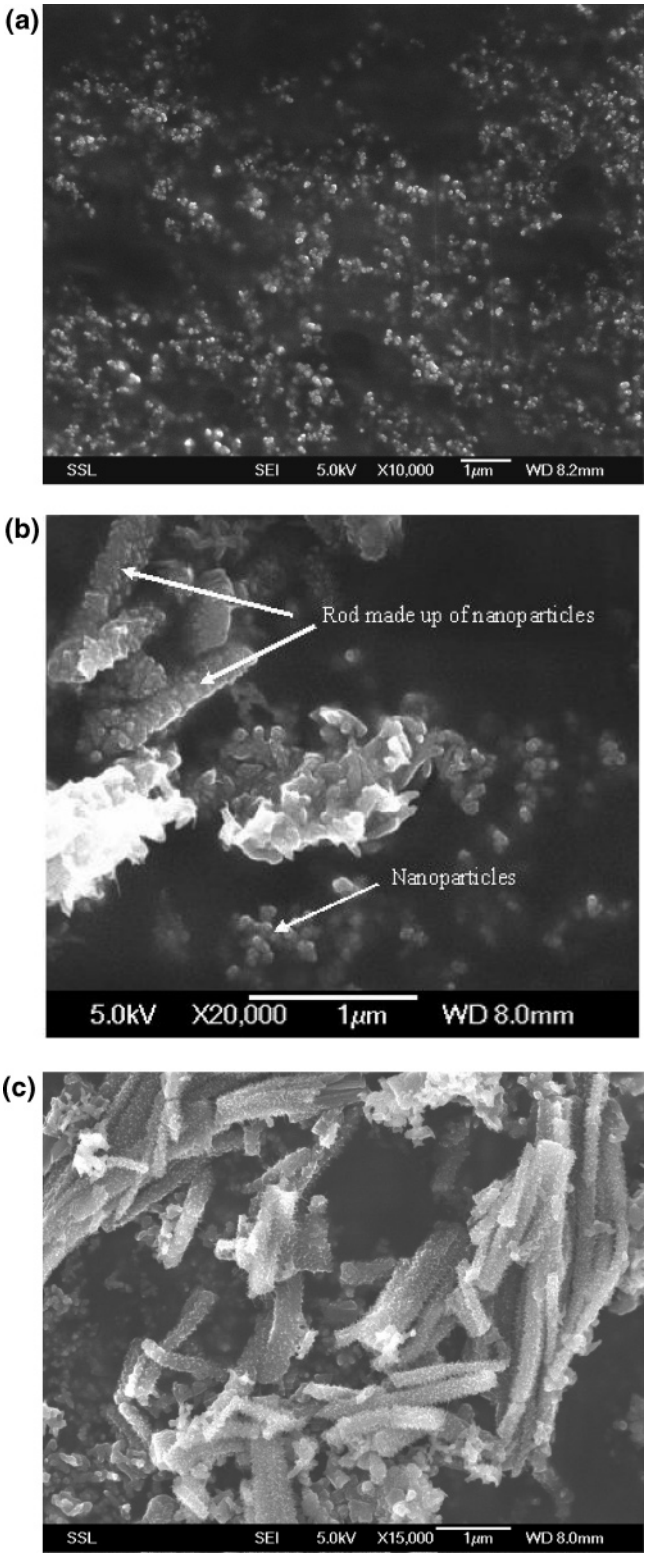

Figure 5. SEM images of PANI at different stages of polymerization. (a) after 35 min of polymerization, (b) after 1.5 h of polymerization, and (c) after 4 h of polymerization. ([An]/[ARAC] = 25, [An] = 0.11 M, [An]/[APS] = 1, temperature = 2.5 °C.)

The solvent-subtracted scattering intensity normalized by its value at the scattering angle $\theta = 30°$ is plotted as a function of the wave vector, $q = (4\pi n/\lambda)\sin(\theta/2)$, where n is the refractive index of the solvent and λ is the wavelength of the light used. The data are quite scattered, which may be attributed to the low concentration used to avoid multiple scattering and the high polydispersity of the sample. As the SEM/TEM images suggest

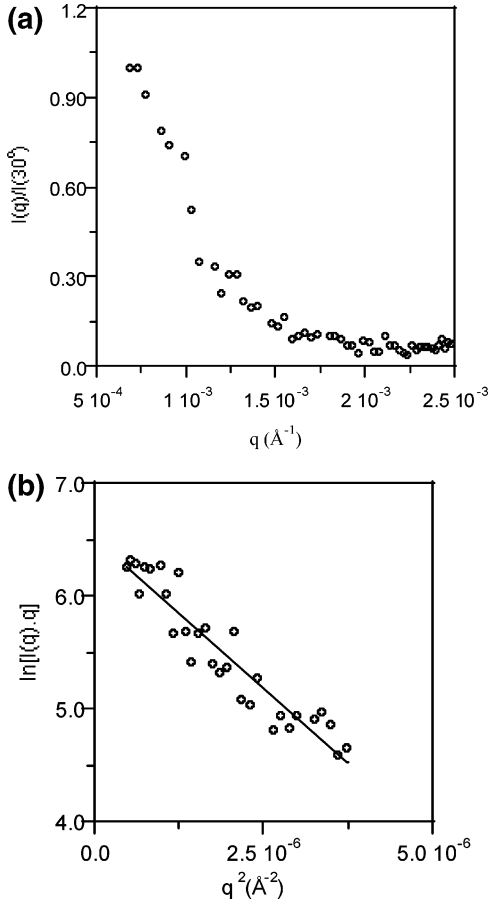

Figure 6. Intensity distribution of SLS data for the nanorods formed using [An]/[ARAC] = 25 with [An] = [APS] = 0.11 M, after 9 h of polymerization at 2.5 °C. The solution was diluted 500 times and equilibrated at 10 °C.

the lengths of the rods to be in micrometers, the SLS data cannot be used to determine the rod length. In the limit of long rods, i.e., $L \gg R$, the scattered intensity can be separated into two components,[40] each corresponding, respectively, to the length effect and rod cross section. For a uniform rod of radius R, the rod cross-section component is

$$I(q) \propto \left(\frac{L}{q}\right)\frac{R^4}{4}\exp(-q^2R^2/4) \tag{5}$$

The above approximation is valid for low-angle parts of the rod scattering curves and suggests that a plot of $\ln[I(q)q]$ versus q^2 will contain a linear (Guinier) region whose slope is equal to $R^2/4$. In Figure 6b, this method of plotting the SLS data is used to obtain the radii of the nanorods. The regression coefficient of the linear fit is 0.94, and the mean radius estimated is 1450 Å (145 nm). The CONTIN program used to analyze the DLS data collected at 90° suggests the existence of huge particles of predominantly two diffusion coefficients centered at 3.0×10^{-11} and 1.44×10^{-9} cm^2 s^{-1}. Assuming the former to be due to larger aggregates, the diffusion coefficient $D = 1.44 \times 10^{-9}$ cm^2 s^{-1} is used to estimate the length of a single rod. For a rod with length-to-diameter ratio p, the translational diffusion coefficient for $400 \geq p \geq 9$ is given by[41]

$$D = \frac{k_B T}{3\pi\eta L}\left\{\ln p + \frac{1}{2}\left[-0.08 + 7.4\left(\frac{1}{\ln 2p} - 0.34\right)^2 + 4.2\left(\frac{1}{\ln 2p} - 0.39\right)^2\right]\right\} \tag{6}$$

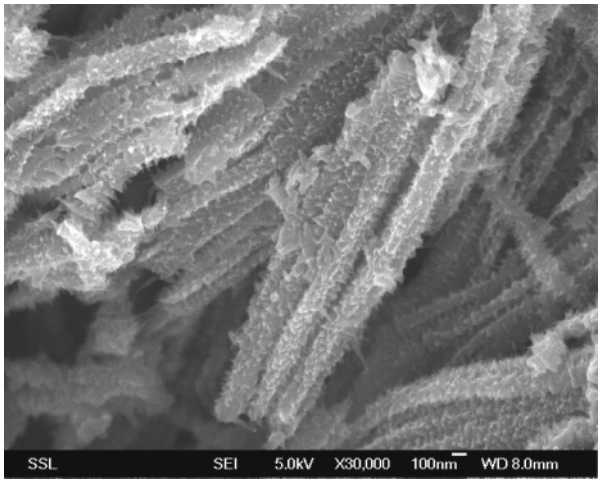

Figure 7. SEM image of PANI nanoparticle nanorods. (Sample conditions are the same as in Figure 1c except the temperature of 10 °C.)

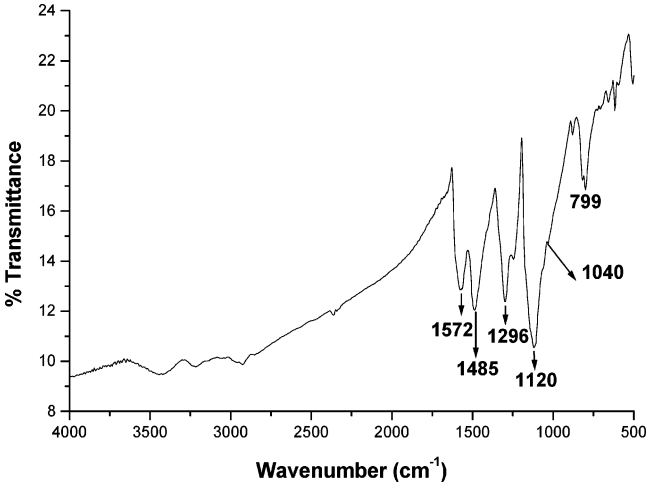

Figure 8. FTIR spectrum of oriented PANI nanoparticle nanorods. (Sample conditions are the same as in Figure 1c.)

where k_B is the Boltzmann constant, T is the temperature of the sample, and η is the viscosity of the solvent. By substitution of the mean diameter obtained from SLS data in the above equation, the rod length is estimated to be 7 μm. For such long rods, the effect of rotational diffusion cannot be ignored. These limitations notwithstanding, the light scattering data analysis gives supportive evidence to the formation of the PANI nanorods by an elongation process.

Self-assembly processes are governed by a balance of entropic and enthalpic effects,[2] which should be strongly temperature-dependent. This temperature dependency would be expected to yield larger aggregate structures through self-assembly of nanoparticles at lower temperatures.[2,4,42] The diameters of the nanoparticle nanorods at different temperatures were consistent with this prediction. At 2.5 °C, we observed the large nanoparticle nanorods with diameters in the range 200−400 nm (Figure 1c). At 10 °C, the nanoparticle nanorods with diameters of 80−120 nm were formed (Figure 7). The oriented nanoparticle nanorod clusters can be prepared favorably at low temperatures, and a mixture of PANI nanostructures would be obtained when the reaction temperature is higher than 10 °C.

Structural Characterization. The molecular structure of PANI nanorods was characterized by FTIR spectroscopy. The FTIR spectrum (Figure 8) shows the characteristic peaks of PANI around 1572, 1485, 1296, 1120, and 799 cm^{-1}. The shifts of the vibration bands (C═C stretching deformation of quinoid[44] shifted from 1590 [45] to 1572 cm^{-1} and that of the benzenoid ring[44] from 1502 [45] to 1485 cm^{-1}) of the PANI nanorod backbone indicate longer effective conjugation lengths.[45] The bands at 1040 and 506 cm^{-1} can be assigned to the absorption of the sulfonate anion[46] from ARAC.

In the UV−vis absorption spectrum, the peaks are observed around 308 and 452 nm, which can be assigned to the $\pi-\pi^*$ transition and the polaron band transition of the PANI backbone, respectively (Figure 9a).[47,48] The band at about 1080 nm is assigned to the polaron transition, which is attributed to the emeraldine salt form of PANI.[49] The red shift of the polaron transition band from 840 to 1080 nm (Figure 9b) is due to the longer conjugation length in the oriented PANI nanorods in comparison with the PANI−HCl products prepared by conventional methods. The peak around 452 nm disappeared for the dedoped PANI nanorods. Instead, the peak around 630 nm assigned to the quinoid unit appeared (Figure 9c).

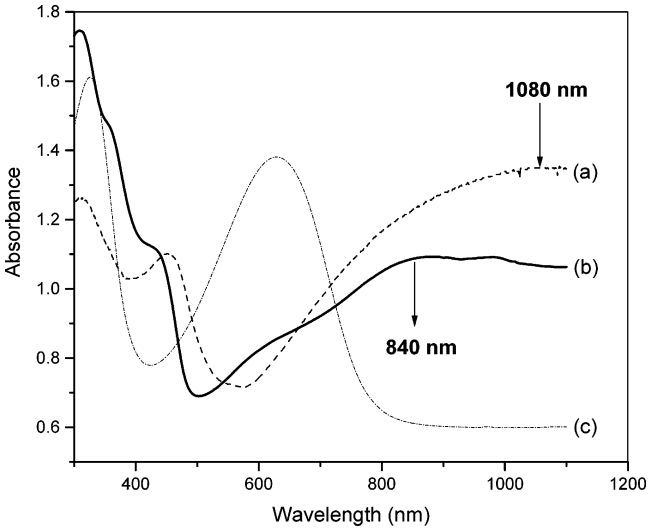

Figure 9. UV−vis spectra of PANI nanostructures dispersed in water: (a) PANI−ARAC (doped); (b) PANI−HCl (doped); (c) PANI−ARAC (dedoped). Sample conditions are the same as in Figure 1c for parts a and c. For part b, the sample conditions are the same as in Figure 1c except that no ARAC has been used.

Conclusion

In conclusion, we report the formation of oriented PANI nanorods made up of nanoparticles and show the utility of self-assembly in generating such a novel material. The oriented nanorods are in the range of 80−400 nm in diameter and 8−15 μm in length. It was found that the morphologies and sizes of the PANI nanorods strongly depend on the ratio of aniline to ARAC, the concentration of aniline, and the reaction temperature. On the basis of the results obtained from the SAXS study, we suggest that rodlike micellar arrays of ARAC−An are responsible for directing the formation of oriented PANI nanoparticle nanorods. The formation of the PANI nanorods by an elongation process was supported by the SEM images and the data analysis of SLS and DLS. It appears that the process involves not only the in situ formation of well-ordered arrays of PANI nanorods but also the simultaneous formation of oriented PANI nanorods with nanoparticle morphologies. The process described here is simple and can be extended to prepare more complex nanostructures with controlled morphologies, orientations, and new surface architectures.

Acknowledgment. We thank Associate Professor Lin Jianyi for his assistance with SEM and the National University of Singapore for financial support.

Supporting Information Available: SEM images of PANI nanotubes in a bundle and rod networks. This material is available free of charge via the Internet at http://pubs.acs.org.

References and Notes

(1) Tian, Z. R.; Voigt, J. A.; LIU, J.; Mckenzie, B.; Mcderott, M. J.; Rodriguze, M. A.; Konishi, H.; Xu, H. F. *Nat. Mater.* **2004**, *2*, 821.

(2) Boal, A. K.; Ilhan, F.; DeRouchey, J. E.; Albrecht, T. T.; Russell, T. P.; Rotello, V. M. *Nature* **2000**, *404*, 746.

(3) Li, M.; Schnablegger, H.; Mann, S. *Nature* **1999**, *402*, 393.

(4) Mann, S.; Shenton, W.; Davis, S. A. *Adv. Mater.* **1999**, *11*, 449.

(5) Weller, H.; Pacholski, C.; Kornowski, D. A. *Angew. Chem., Int. Ed.* **2002**, *41*, 1188.

(6) Behrens, S.; Habicht, W.; Dinjus, E.; Rahn, K.; Böhm, K. J.; Unger, E.; Rösner, H. *Adv. Mater.* **2002**, *14*, 1621.

(7) Leontidis, E.; Orphanou, M.; Leodidou, T. K.; Krumeich, K.; Caseri, W. *Nano Lett.* **2003**, 3569.

(8) Mirkin, C. A.; Li, Z.; Chung, S. W.; Nam, J. M.; Ginger, D. S. *Angew. Chem., Int. Ed.* **2003**, *42*, 2306.

(9) Himmelhaus, M.; Kaltenpoth, G.; Grunze, M.; Slansky, L.; Caruso, F. *Adv. Mater.* **2003**, *15*, 1113.

(10) Chen, S. A.; Lee, T. S. *J. Polym. Sci., Part C: Polym. Lett.* **1987**, *25*, 455.

(11) Desilvestro, J.; Scheifele, W. *J. Mater. Chem.* **1993**, *3*, 263.

(12) Martin, C. R. *Chem. Mater.* **1996**, *8*, 1739.

(13) Parthasarathy, R. V.; Martin, C. R. *Chem. Mater.* **1994**, *6*, 1627.

(14) Wu, C. G.; Bein, T. *Science* **1994**, *264*, 1757.

(15) Wei, Z. X.; Zhang, Z. M.; Wan, M. X. *Langmuir* **2002**, *18*, 917.

(16) Yang, Y. S.; Wan, M. X. *J. Mater. Chem.* **2002**, *12*, 897.

(17) Choi, S. J.; Park, S. M. *Adv. Mater.* **2000**, *12*, 1547.

(18) Liu, J. M.; Yang, S. C. *Chem. Commun.* **1991**, 1529.

(19) Wei, Z.; Wan, M. X.; Lin, T.; Dai, L. M. *Adv. Mater.* **2003**, *15*, 136.

(20) Huang, K.; Wan, M. X. *Chem. Mater.* **2002**, *14*, 3486.

(21) Qiu, H. J.; Wan, M. X.; Matthews, B.; Dai, L. M. *Macromolecules* **2001**, *34*, 675.

(22) Xia, H.; Chan, H. S. O.; Xiao, C. Y.; Cheng, D. M. *Nanotechnology* **2004**, *15*, 1807.

(23) Huang, W. S.; Humphrey, B. D.; MacDiarmid, A. G. *J. Chem. Soc., Faraday Trans.* **1986**, *82*, 2385.

(24) Hassan, P. A.; Sawant, S. N.; Bagkar, N. C.; Yakhmi, J. V. *Langmuir* **2004**, *18*, 2543.

(25) Hous, G. In *Anionic Surfactant Organic Chemistry*; Stache, H. W., Ed.; Marcel Dekker: New York, 1995; Vol. 56, p 82.

(26) Bocjstaller, M.; Köhler, W.; Wegner, G.; Vassopoulos, D.; Fytas, G. *Macromolecules* **2000**, *33*, 3951.

(27) Hirose, G.; Sepulveda, L. *J. Phys. Chem.* **1981**, *85*, 3689.

(28) Zhang, Z.; Wei, Z.; Wan, M. X. *Macromolecules* **2002**, *35*, 5937.

(29) Wei, Z.; Wan, M. X. *J. Appl. Polym. Sci.* **2003**, *87*, 1297.

(30) Langer, J. J. *Adv. Mater. Opt. Electron.* **1999**, *9*, 1.

(31) (a) Li, Z.; Chung, S. W.; Nam, J. M.; Ginger, D. S.; Mirkin, C. A. *Angew. Chem., Int. Ed.* **2003**, *42*, 2306. (b) Bahceci, S.; Toppare, L.; Yurtsever, E. *Synth. Met.* **1994**, *68*, 57. (c) Zheng, W. Y.; Wang, R. H.; Levon, K.; Rong, Z. Y.; Taka, T.; Pan, W. *Macromol. Chem. Phys.* **1995**, *196*, 2443. (d) Kosonen, H.; Ruokolainen, J.; Knaapila, M.; Torkkeli, M.; Jokela, K.; Serimaa, R.; Brinke, G.; Bras, W.; Monkman, A. P.; Ikkala, O. *Macromolecules* **2000**, *33*, 8671.

(32) (a) Zhang, L.; Wan, M. X. *Adv. Funct. Mater.* **2003**, *13*, 815. (b) Zhang, L.; Long, Y.; Chen, Z.; Wan, M. X. *Adv. Funct. Mater.* **2004**, *14*, 693.

(33) (a) Ruokolainen, J.; Mäkinen, R.; Torkkeli, M.; Mäkelä, T.; Serimaa, R.; ten Brinke, G.; Ikkala, O. *Science*, **1998**, *280*, 557. (b) Ikkala, O.; ten Brinke, G. *Science* **2002**, *295*, 2407. (c) Behrens, S.; Habicht, W.; Dinjus, E.; Rahn, K.; Böhm, K. J.; Unger, E.; Rösner, H. *Adv. Mater.* **2002**, *14*, 1621.

(34) (a) Sadasivan, S.; Fowler, C. E.; Khushalani, D.; Mann, S. *Angew. Chem., Int. Ed.* **2002**, *41*, 2151; (b) Sadasivan, S.; Khushalani, D.; Mann, S. *J. Mater. Chem.* **2003**, *13*, 1023.

(35) Clint, J. H. *Surfactant Aggregation*; Blackie, Chapman and Hall: Glasgow, U. K., New York, 1991.

(36) Ikkala, O.; Brinke, G. *Chem. Commun.* **2004**, 2131.

(37) Huang, J.; Kaner, R. B. *Angew. Chem., Int. Ed.* **2004**, *43*, 5817.

(38) Harada, M.; Adachi, M. *Adv. Mater.* **2000**, *12*, 839.

(39) Guinier, A.; Fournet, G. *Small-Angle Scattering of X-Rays*; Wiley: New York, 1955.

(40) Glatter, O.; Kratky, O. *Small-Angle X-Ray Scattering*; Academic: London, U. K. 1982.

(41) Tirado, M. M.; Martinez, C. L.; Torre, J. G. *J. Chem. Phys.* **1984**, *81*, 2047.

(42) Deans, R.; Ilhan, F.; Rotello, V. M. *Macromolecules* **1999**, *32*, 4956.

(43) Lahav, M.; Sehayek, T.; Vaskevich, A.; Rubinstein, I. *Angew. Chem., Int. Ed.* **2003**, *42*, 5576.

(44) Chen, S. A.; Lee, H. T. *Macromolecules* **1995**, *28*, 2858.

(45) Wang, Y.; Rubner, M. F. *Synth. Met.* **1992**, *47*, 255.

(46) Chen, S. A.; Hwang, G. W. *J. Am. Chem. Soc.* **1995**, *117*, 10055.

(47) Yue, J.; Epstein, A. J. *J. Am. Chem. Soc.* **1990**, *112*, 2800.

(48) Yue, J.; Wang, Z. H.; Cromack, K. R.; Epstein, A. G.; MacDiarmid, A. G. *J. Am. Chem. Soc.* **1991**, *113*, 2665.

(49) Cao, Y.; Smith, P.; Heeger, A. J. *Synth. Met.* **1989**, *32*, 263.